

Accepted Manuscript

Structure Guided Optimization of a Fragment Hit to Imidazopyridine Inhibitors of PI3K

Sabina Pecchi, Zhi-Jie Ni, Wooseok Han, Aaron Smith, Jiong Lan, Matthew Burger, Hanne Merritt, Marion Wiesmann, John Chan, Susan Kaufman, Mark S. Knapp, Johanna Janssen, Kay Huh, Charles F. Voliva

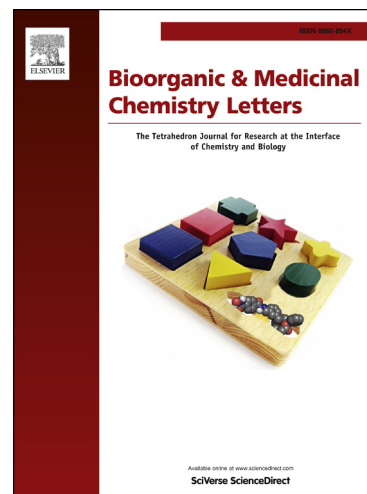
PII: S0960-894X(13)00719-1
DOI: <http://dx.doi.org/10.1016/j.bmcl.2013.06.010>
Reference: BMCL 20574

To appear in: *Bioorganic & Medicinal Chemistry Letters*

Received Date: 1 April 2013
Revised Date: 30 May 2013
Accepted Date: 3 June 2013

Please cite this article as: Pecchi, S., Ni, Z.-J., Han, W., Smith, A., Lan, J., Burger, M., Merritt, H., Wiesmann, M., Chan, J., Kaufman, S., Knapp, M.S., Janssen, J., Huh, K., Voliva, C.F., Structure Guided Optimization of a Fragment Hit to Imidazopyridine Inhibitors of PI3K, *Bioorganic & Medicinal Chemistry Letters* (2013), doi: <http://dx.doi.org/10.1016/j.bmcl.2013.06.010>

This is a PDF file of an unedited manuscript that has been accepted for publication. As a service to our customers we are providing this early version of the manuscript. The manuscript will undergo copyediting, typesetting, and review of the resulting proof before it is published in its final form. Please note that during the production process errors may be discovered which could affect the content, and all legal disclaimers that apply to the journal pertain.



Structure Guided Optimization of a Fragment Hit to Imidazopyridine Inhibitors of PI3K

Sabina Pecchi^a, Zhi-Jie Ni^a, Wooseok Han^{a*}, Aaron Smith^a, Jiong Lan^a, Matthew Burger^a, Hanne Merritt^b, Marion Wiesmann^c, John Chan^b, Susan Kaufman^b, Mark S. Knapp^a, Johanna Janssen^a, Kay Huh^a, and Charles F. Voliva^b

^aGlobal Discovery Chemistry/Oncology and Exploratory Chemistry, Novartis Institutes for Biomedical Research, Emeryville, CA, U.S.A., ^bOncology, Novartis Institutes for Biomedical Research, Emeryville, CA, U.S.A., ^cOncology DA, Novartis Institutes for Biomedical Research, Basel, Switzerland

Received Month XX, 2013; Accepted Month XX, 2013

Abstract—PI3 Kinases are a family of lipid kinases mediating numerous cell processes such as proliferation, migration and differentiation. The PI3 Kinase pathway is often de-regulated in cancer through PI3K α overexpression, gene amplification, mutations and PTEN phosphatase deletion. PI3K inhibitors represent therefore an attractive therapeutic modality for cancer treatment. Herein we describe how the potency of a benzothiazole fragment hit was quickly improved based on structural information and how this early chemotype was further optimized through scaffold hopping. This effort led to the identification of a series of 2-acetamido-5-heteroaryl imidazopyridines showing potent *in vitro* activity against all class I PI3Ks and attractive pharmacokinetic properties.

©2000 Elsevier Science Ltd. All rights reserved.

* Corresponding author. Tel.: +1(510) 923-2848; Fax: +1(510) 923-3360; E-mail: wooseok.han@novartis.com

Phosphatidylinositol 3-kinases (PI3Ks) are a family of lipid and serine/threonine kinases involved in a diverse set of cellular functions.¹ PI3Ks can be categorized in class I, II or III, depending on their subunit structure, regulation and substrate selectivity.² Class IA PI3Ks are heterodimers composed of a catalytic p110 subunit (α , β and δ isoforms) constitutively associated with a regulatory subunit that can be p85 α , p55 α , p50 α , p85 β or p55 γ . The Class IB has one family member, a heterodimer composed of a catalytic p110 γ subunit associated with one of two regulatory subunits, p101 or p84. Class IA PI3Ks are activated by tyrosine kinases while Class IB is activated by G protein-coupled receptors, therefore linking upstream receptors with downstream cellular activities including cell growth, proliferation, survival, chemotaxis, cellular trafficking, membrane ruffling and glucose homeostasis,¹ motility, metabolism, inflammatory and allergic responses, transcription and translation.^{2,3} PI3Ks catalyze the transfer of phosphate to the D-3' position of inositol lipids to produce phosphoinositol-3-phosphate (PIP), phosphoinositol-3,4-diphosphate (PIP₂) and phosphoinositol-3,4,5-triphosphate (PIP₃), second messengers in numerous signaling cascades.⁴ In many cases, PIP₂ and PIP₃ recruit AKT to the plasma membrane where it acts as a nodal point for many intracellular signaling pathways important for growth and survival.^{5,6} Aberrant regulation of PI3K, which often increases survival through AKT activation, is one of the most prevalent events in human cancer⁷ and can occur at multiple levels.^{8,9} In particular, p110 α pathway deregulation has been demonstrated in ovarian, breast, colon and brain cancers.^{10,11} These observations support the inhibition of Class I PI3 kinases as a potential treatment for a variety of tumor types and other proliferative diseases,^{12,13} hence the interest during the last ten years in generating suitable molecules to test this hypothesis in the clinic.^{14,15,16,17,18}

In the course of our efforts to identify a backup series for our 2-morpholino pyrimidines front runners¹⁹ and NVP-BKM120 (**1**, Fig. 1),²⁰ we conducted a second HTS campaign on an expanded compound collection and fragment library. Through this effort, several hits were identified and compound **2** (a fragment with MW = 250.2, Fig. 1) was selected for follow up. Compound **2** had reasonable potency against PI3K α and good ligand efficiency (IC₅₀ = 2.2 μ M, LE = 0.47). It appeared to be approximately equipotent

against the γ isoform and less potent against the β and δ isoforms, PI4K and VPS34.²¹ We were therefore intrigued by the opportunity to explore this selectivity potential.

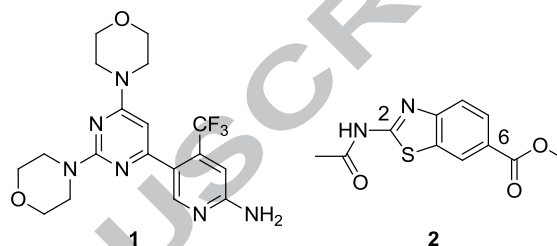


Figure 1. Clinical candidate **1** (NVP-BKM120) and benzothiazole fragment hit **2**

In silico profiling of **2** (PSA = 96, cLogP = 2.0, LogD_{7.4} = 1.5, 1 HBD, 3 HBA, good predicted passive permeability) did not show any significant alerts. One significant advantage in the follow up was the availability of a co-crystal structure of **2** in p110 γ , obtained shortly after hit triaging.

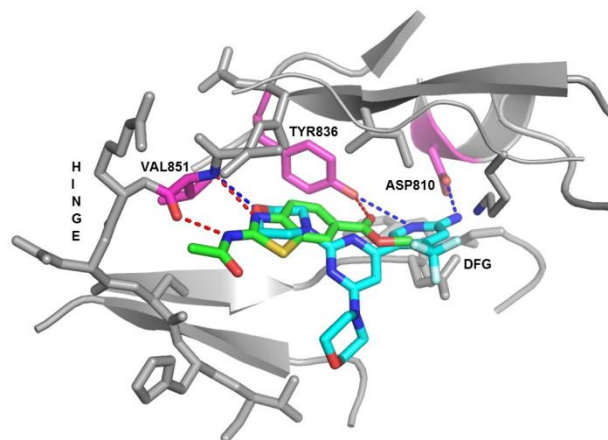
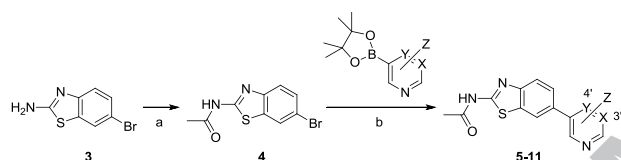


Figure 2. Model of compound **2** and NVP-BKM120 (**1**) in p110 α .

Fig. 2 shows an overlay of compound **2** with NVP-BKM120 (**1**, Fig. 1), the lead compound from the 2-morpholinopyrimidine series,²⁰ in a homology model of p110 α . This model was generated based on the co-crystal structures of both compounds in p110 γ .²² It is worth noting that the 2-acetamidobenzothiazole scaffold provides one additional contact with the hinge binding domain of the ATP binding site in comparison to the morpholine. The acetamide NH acts as a H bond donor and the benzothiazole N acts as a H bond

acceptor with VAL851 backbone carbonyl and NH, respectively. The third hydrogen bond interaction is provided by the carbonyl of the ester substituent in the 6-position with the OH of TYR836. The benzothiazole spans two key regions of the active site (hinge domain and catalytic region) more efficiently than the 2-morpholinopyrimidine series, where the central pyrimidine ring has mainly a scaffolding function. The ester interaction is likely inefficient, but the 6-position of the benzothiazole provides a good vector for growth in the direction of the “affinity pocket”, accessing the same area of the binding site as the one occupied by the aminopyridine in the 2-morpholinopyrimidine series. This indicated the potential for hybridizing the two chemotypes.

We therefore proceeded to synthesize a series of benzothiazoles having 6-membered rings at the 6-position. The analogs were easily obtained from commercially available 2-amino-6-bromo benzothiazole **3** by acetylation and Suzuki coupling with various heterocyclic boronic esters, either commercially available or synthesized as previously described²³ (Scheme 1).



Scheme 1. Synthesis of 6-heteroaryl substituted 2-acetamido benzothiazoles. Reagents and conditions: (a) Ac₂O, THF, r.t.; (b) 2M Na₂CO₃, Pd(dppf)Cl₂·CH₂Cl₂, DME, microwave, 115°C, 10 min.

Some of the results obtained are summarized in Table 1.

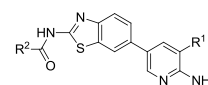
#	R	PI3K α IC ₅₀	pAKT ^{S607/473} IC ₅₀	Prol. EC ₅₀	#	R	PI3K α IC ₅₀	pAKT ^{S607/473} IC ₅₀	Prol. EC ₅₀
2		2.2	ND	ND	8		2.0	ND	ND
5		0.11	0.50	9.7	9		0.0079	0.08	0.41
6		0.063	0.14	2.9	10		0.036	0.30	2.5
7		0.054	0.19	1.3	11		0.033	0.11	0.67

Table 1. Position 6- SAR in the benzothiazole series. IC₅₀ and EC₅₀ in μ M. Cell line: A2780 ovarian carcinoma.

Replacement of the ester in compound **2** with a 3-pyridyl (**5**) gave a 20-fold potency improvement in the biochemical assay, and showed some pathway modulation (IC₅₀ for the inhibition of AKT phosphorylation on SER473 in the A2780 ovarian

carcinoma cell line was 0.5 μ M). Aminopyridine **6** maintained high Ligand Efficiency (LE = 0.5) and was almost 35-fold more potent than **2**. Consequently, mechanism modulation was enhanced to a level sufficient to observe a signal in our functional assay (inhibition of cell proliferation EC₅₀ = 2.9 μ M). Interestingly, aminopyrimidine **7** was comparable to **6**, indicating that the SAR was not tracking with the earlier 2-morpholinopyrimidine series, where 6-aminopyrimidine analogs were 50 to 100-fold more potent than the pyridines.¹⁹ Furthermore, a CF₃ group in the 4'-position of **8**, the preferred position for substitution in the 2-morpholinopyrimidine series,^{19,20} was not tolerated. On the other hand, various substituents were tolerated in the 3'-position (e.g. **9-11**). The 3'-CF₃ analog **9** was the most potent with almost 10-fold biochemical potency improvement compared to **6** and with a 2- and 7-fold improvement in mechanism modulation and inhibition of cell proliferation, respectively. It is worth noting, however, that neither LE nor LLE (0.47 and 4.9) were improved for **9** compared to **6** (LLE = 4.8).

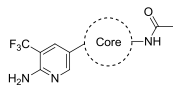
Thus, this hybridization approach led to the quick identification of novel, potent PI3K α inhibitors. Potency against the other isoforms was also improved, and the series was not as selective as initially observed for compound **2** (e.g. PI3K β IC₅₀ was 0.030 μ M for **6**) but was still an interesting starting point for pan Class I PI3K inhibitors. Both compounds **6** and **9** had good microsomal stability and permeability, with low efflux potential in the Caco-2 assay.²⁴ The compounds were advanced to rat PK (Table 5) where they demonstrated oral exposure. However, based on our understanding of PK/PD efficacy relationship in this series, this exposure would not have sufficed for inhibiting tumor growth in our in vivo mouse xenograft model. In addition, low solubility (4.2 and 1.5 μ M) and CYP450 inhibition (IC₅₀ for 3A4 = 0.05 and 0.8 μ M) were significant issues. To address solubility, we introduced basic amines in the 2-position (solvent exposed). Some of the results are shown in Table 2. We observed potency loss, but to a lesser extent when more than one carbon tether was introduced on the amide (compare **6** with **13**), and up to 80-fold improvement in solubility (**6** vs. **14**). Tracking with the 2-acetamido series, the 3'-CF₃ aminopyridines were more potent than the unsubstituted aminopyridines (10 to 20-fold, **14** vs. **13**). Morpholine was also used as solubilizing group (compound **15**), but was less effective. Due to lower efficiency (no potency improvement accompanied the increase in MW) and increased efflux potential (e.g. Caco-2 for compound **11** = A-B 6.7, B-A 18, B/A 2.7), this series was promptly abandoned.



#	R ₁	R ₂	PI3K α IC ₅₀	pAKT ^{Ser473} IC ₅₀	Prol. EC ₅₀	Solubility
6	H	CH ₃	0.063	0.14	2.9	4.2
9	CF ₃	CH ₃	0.0079	0.08	0.41	1.5
12	H	CH ₂ -N ₆	1.2	ND	ND	7.1
13	H	(CH ₂) ₂ -N ₆	0.26	0.36	5.9	28
14	CF ₃	(CH ₂) ₂ -N ₆	0.014	0.11	1.8	56
15	CF ₃	(CH ₂) ₂ -N ₄	0.025	0.15	4.1	8.3

Table 2. Variations on the acetamide for solubility improvement. IC₅₀, EC₅₀ and solubility (PBS) in μ M (pH 7.4). Cell line: A2780 ovarian carcinoma.

A strategy focused on modifications of the core structure was then undertaken. In particular, a series of 5,6- and 6,6-fused heterocycles were explored as benzothiazole replacements and some results are shown in Table 3.



#	Core	PI3K α IC ₅₀	pAKT ^{Ser473} IC ₅₀	Prol. EC ₅₀	cLogp	Solubility
9		0.008	0.08	0.41	3.1	1.5
16		0.002	0.020	0.42	1.7	1.0
17		0.004	0.079	1.1	2.4	5.7
18		0.11	ND	>10	1.8	1.0
19		0.79	ND	>10	2.4	1.3
20		1.6	ND	>10	1.8	0.5
21		3.8	ND	ND	1.6	4.8
22		4.0	ND	ND	2.6	25

Table 3. Scaffold hopping around the benzothiazole core. IC₅₀, EC₅₀ and solubility (PBS) in μ M (pH 7.4). Cell line: A2780 ovarian carcinoma.

Most of the core variations led to significant potency decrease, with the exception of imidazopyridazine **16**, demonstrating a 4-fold potency increase compared to **9**, and imidazopyridine **17**, which maintained potency. Compound **17** offered the best potency/solubility balance, and was investigated further. Compound **17** was potent against all PI3K isoforms, including the most common p110 α mutations, and showed mechanism modulation and inhibition of cell proliferation in a series of cell lines with PI3K pathway deregulation (Table 4). It was stable in rat and human microsomes had good permeability with low efflux potential,²⁴ and addressed the CYP liabilities of the benzothiazole scaffold (IC₅₀

>25 μ M against CYP450 3A4, 1A2, 2D6, 2C9, and 2C19).

The synthesis of compound **17** is shown in Scheme 2.²⁵ Tosylation of 2-amino-4-iodopyridine and N-alkylation with iodo acetamide led to intermediate **24** which cyclized upon treatment with TFAA. The resulting imidazopyridine 2-trifluoroacetamide was deprotected with potassium carbonate and the 2-amino group was acetylated, to give 5-I derivative **25**. Compound **25** was then coupled with 5-(4,4,5,5-tetramethyl-1,3,2-dioxaborolan-2-yl)-3-(trifluoromethyl)pyridin-2-amine **26** under Suzuki conditions²³ to give the desired compound **17**.

Biochemical Profile (IC₅₀, μ M)

PI3K α	PI3K α E542K	PI3K α H1047R	PI3K γ
0.0036	0.0059	0.012	0.0082
PI3K β	PI3K δ	PI4K β	VPS34
0.27	0.1	2.35	1.8

Cellular Profile (EC₅₀, μ M)

Cell line	pAKT ^{S473}	pAKT ^{T308}	Proliferation
A2780	0.079	<0.041	1.1
U87MG	0.050	<0.041	2.0
T47D	0.034	ND	1.3

Table 4. *In vitro* profile of compound **17**.

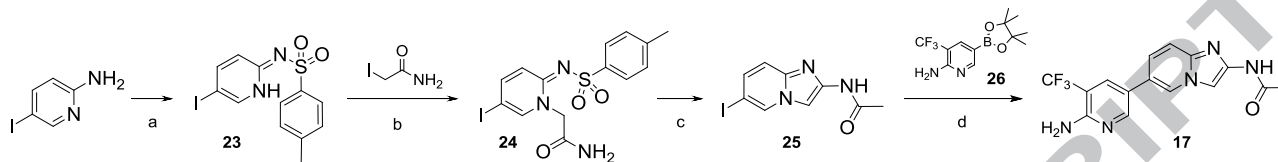
The co-crystal structure of **17** with p110 γ ²⁶ gave further insights in the binding mode (Fig. 3). The nitrogen atom in the imidazopyridine core forms a hydrogen bond with VAL882 backbone NH, and the 2-acetamide NH forms an interaction with VAL882 backbone carbonyl, as expected. The endocyclic N of the 5-aminopyridine substituent functions as H bond acceptor with TYR867 OH and the NH₂ donates to ASP964. Compared to the morpholino pyrimidine scaffold (Fig. 2),¹⁹ this substituent is not buried as deep in the catalytic region, but the CF₃ group fits in the same hydrophobic pocket, accessing it through a different vector. Substituents in 4'-position are not tolerated because this position does not provide the right trajectory to the same hydrophobic pocket. In addition, the imidazopyridine and aminopyridine rings need to be almost coplanar for a favorable binding conformation and a 4'-substituent causes a significant deviation from planarity.

It is worth noting that compared to **6** and **9**, compound **17** shows improved LLE retaining LE (6.0 and 0.49, respectively). This suggests that while the potency improvement in **9** may be solely driven by increased LogP, compound **17** can achieve a similar potency in a more polar property space, likely through a better interaction with the hinge domain, hence the improved LLE.

Compound **17** showed attractive rat PK properties with low clearance and V_{ss}, and oral AUC approximately 10-fold higher than its benzothiazole analog **9** (Table 5).

#	IV			%F	PO	
	VSS (L/Kg)	CL (mL/min/Kg)	t _{1/2} (h)		AUC (μM ^h)	C _{MAX} (μM)
6	3.6	19	2.5	57	16	2.5
9	ND	ND	ND	ND	18	2.9
17	0.68	2	3	95	198	15.7

Table 5. Rat PK properties for benzothiazoles **6** and **9** and imidazopyridine **17** (doses: 5 mg/kg IV and 10 mg/kg PO).



Scheme 2. Synthesis of compound **17**. Reagents and conditions: (a) TsCl, Pyridine, 90 °C, 16 h; (b) Hunig's base, DMF, r.t., 24 h; (c) i: TFAA, DCM, reflux, 3 h; ii: K₂CO₃, MeOH, 90 °C, 16 h; iii: Acetic anhydride, pyridine, r.t.; (d) Pd(dppf)Cl₂·CH₂Cl₂, DME, 2M Na₂CO₃, 120 °C, microwave, 10 min.

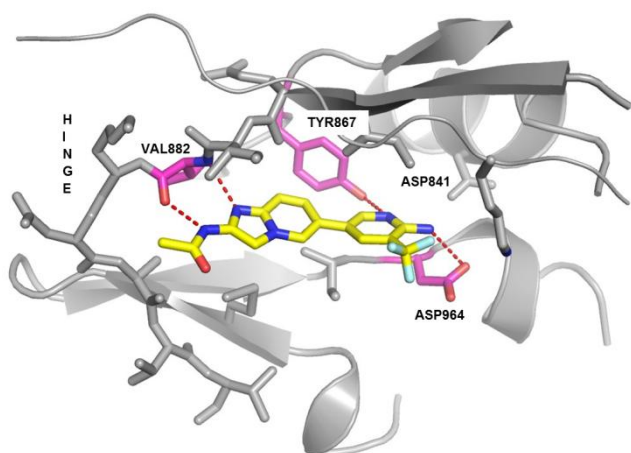


Figure 3. Co-crystal structure of compound **17** with PI3K γ . Key interactions are indicated by dotted lines.

In conclusion, structural information on the benzothiazole fragment hit **2** and hybridization with a known chemotype allowed rapid biochemical and cell potency optimization. Subsequently, a survey of

References and Notes

- Engelman, J. A.; Luo, J.; Cantley, L. C. *Nat. Rev. Genet.* **2006**, *7*, 606.
- Katso, R.; Okkenhaug, K.; Ahmadi, K.; White, S.; Timms, J.; Waterfield, M. D. *Annu. Rev. Cell Dev. Biol.* **2001**, *17*, 615.
- Wymann, M. P.; Zvelebil, M.; Laffargue, M. *Trends Pharmacol. Sci.* **2003**, *24*, 366.
- Vanhaesebroeck, B.; Leever, S. J.; Ahmadi, K.; Timms, J.; Katso, R.; Driscoll, P. C.; Woscholski, R.; Parker, P. J.; Waterfield, M. D. *Annu. Rev. Biochem.* **2001**, *70*, 535.
- Vanhaesebroeck, B.; Stephens, L.; Hawkins, P. *Nat. Rev. Mol. Cell Biol.* **2012**, *13*, 195.
- Andjelkovic, M.; Alessi, D. R.; Meier, R. *et al. J. Biol. Chem.* **1997**, *272*, 31515.
- Liu, P.; Cheng, H.; Roberts, T. M.; Zhao, J. *Nat. Rev. Drug Disc.* **2009**, *8*, 627.

various 5,6- and 6,6-fused core heterocyclic systems led to the identification of imidazopyridine **17**. This compound had improved potency, solubility and no CYP450 issues compared to the benzothiazoles. Attractive rat pharmacokinetic properties warranted further evaluation. Progress in this class of PI3K inhibitors will be reported in due course.

Acknowledgements

The authors wish to acknowledge Frederic Stauffer and Giorgio Caravatti for help with the *in vitro* profiling of compound **17**, George Thomas for discussing *in vivo* pharmacokinetics and Yongjin Xu for LE and LLE calculations.

Supplementary Data

Supplementary information associated with this article can be found in the on line version at www.sciencedirect.com

- Ali, I. U.; Schriml, L. M.; Dean, M. *J. Natl. Cancer Inst.* **1999**, *91*, 1922.
- Cross, D. A.; Alessi, D. R.; Cohen, P. *et al. Nature* **1995**, *378*, 785.
- Samuels, Y.; Wang, Z.; Bardelli, A.; Silliman, N.; Ptak, J.; Szabo, S.; Yan, H.; Gasdar, A.; Powell, S. M.; Riggins, G. J.; Willson, J. K.; Markowitz, S.; Kinzler, K. W.; Vogelstein, B.; Velculescu, V. E. *Science* **2004**, *304*, 554.
- Leslie, N. R.; Downes, C. P. *Biochem. J.* **2004**, *382*, 1.
- Kong, D.; Yamori, T. *Cancer Sci.* **2008**, *99*, 1734.
- Workman, P.; Clarke, P. A.; Raynaud, F. I.; Van Montfort, R. L. M. *Cancer Res.* **2010**, *70*, 2146.
- Nuss, J. M.; Tshako, A. L.; Anand, N. K. in *Annual Reports in Medicinal Chemistry*; Macor, J. E., Ed.; Academic Press: Oxford, 2009; Vol. 44, p. 339.
- Maira, S.-M.; Stauffer, F.; Brueggen, J.; Furet, P.; Schnell, C.; Fritsch, C.; Brachmann, S.; Chene, P.; De Pover, A.; Shoemaker, K.; Fabbro, D.; Gabriel, D.;

Simonen, M.; Murphy, L.; Finan, P.; Sellers, W.; Garcia-Echeverria, C. *Mol. Cancer Ther.* **2008**, *7*, 1851.

¹⁶ Folkles, A. J.; Ahmadi, K.; Alderton, W. K.; Alix, S.; Baker, S. J.; Box, G.; Chuckowree, I. S.; Clarke, P. A.; Depledge, P.; Eccles, S. A.; Friedman, L. S.; Hayes, A.; Hancox, T. C.; Kugendradas, A.; Lensun, L.; Moore, P.; Olivero, A. G.; Pang, J.; Patel, S.; Pergl-Wilson, G. H.; Raynaud, F. I.; Robson, A.; Saghiri, N.; Salphati, L.; Sohal, S.; Ultsch, M. H.; Valenti, M.; Wallweber, H. J. A.; Wan, N. C.; Wiesmann, C.; Workman, P.; Zhyvoloup, A.; Zvelebil, M. J.; Shuttleworth, S. J. *J. Med. Chem.* **2008**, *51*, 5522

¹⁷ Knight, S. D.; Adams, N. D.; Burgess, J. L.; Chaudhari, A. M.; Darcy, M. G.; Donatelli, C. A.; Luengo, J. E.; Newlander, K. A.; Parrish, C. A.; Ridgers, L. H.; Sarpong, M. A.; Schmidt, S. J.; Van Aller, G. S.; Carson, J. D.; Diamond, M. A.; Elkins, P. A.; Gardiner, C. M.; Garver, E.; Gilbert, S. A.; Gontarek, R. R.; Jackson, J. R.; Kershner, K. L.; Luo, L.; Raha, K.; Sherk, C. S.; Sung, C. M.; Sutton, D.; Tummino, P. J.; Wegrzyn, R. J.; Auger, K. R.; Dhanak, D. *ACS Med. Chem. Lett.* **2010**, *1*, 39.

¹⁸ Courtney, K. D.; Corcoran R. B.; Engelman, J. A. *J. Clin. Oncology*, **2010**, *28*, 1075.

¹⁹ (a) Pecchi, S.; Renhowe, P. A.; Taylor, C.; Kaufman, S.; Merrit, H.; Wiesmann, M.; Shoemaker, K.; Knapp, M. S.; Hendrickson, T. F.; Fantl, W.; Voliva, C. F. *Bioorg. Med. Chem. Lett.* **2010**, *20*, 6895; (b) Burger, M. T.; Knapp, M.; Wagman, A.; Ni, Z. J.; Hendrickson, T.; Atallah, G.; Zhang, Y.; Frazier, K.; Verhagen, J.; Pfister, K.; Ng, S.; Smith, A.; Bartulis, S.; Merrit, H.; Wiesmann, M.; Xin, X.; Haznedar, J.; Voliva, C. F.; Iwanowicz, E.; Pecchi, S. *ACS Med. Chem. Lett.* **2011**, *2*, 34.

²⁰ (a) Burger, M. T.; Pecchi, S.; Wagman, A.; Ni, Z.-J.; Knapp, M.; Hendrickson, T.; Atallah, G.; Pfister, K.; Zhang, Y.; Bartulis, S.; Frazier, K.; Ng, S.; Smith, A.; Verhagen, J.; Haznedar, J.; Huh, K.; Iwanowicz, E.; Xin, X.; Menezes, D.; Merritt, H.; Lee, I.; Wiesmann, M.; Kaufman, S.; Crawford, K.; Chin, M.; Bussiere, D.; Shoemaker, K.; Zaror, I.; Maira, S. -M.; Voliva, C. F. *ACS Med. Chem. Lett.* **2011**, *2*, 774. (b) Maira, S.-M.; Pecchi, S.; Huang, A.; Burger, M.; Knapp, M.; Sterker, D.; Schnell, C.; Guthyl, D.; Nagel, T.; Wiesmann, M.; Brachmann, S.; Fritsch, C.; Dorsch, M.; Chene, P.; Shoemaker, K.; De Pover, A.; Menezes, D.; Martiny-Baron, G.; Fabbro, D.; Wilson, C. J.; Schlegel, R.; Hofmann, F.; Garcia-Echeverria, C.; Sellers, W. R.; Voliva C. F. *Mol. Canc. Ther.* **2012**, *11*, 317.

²¹ PI3K β IC₅₀ = 23 μ M (8), PI3K γ IC₅₀ = 4.2 μ M (1), PI3K δ IC₅₀ = >25 μ M (2), PI4K β IC₅₀ = 10 μ M (4), VPS34 IC₅₀ = >25 μ M (5). Number in parenthesis indicates number of replicates.

²² Structure of NVP-BKM120 (**1**) in PI3K γ submitted under PDB accession code 3SD5. Structure of compound **2** in PI3K γ submitted under PDB accession code **4KZ0**.

²³ Ni, Z.-J.; Pecchi, S.; Burger, M.; Han, W.; Smith, A.; Atallah, G.; Bartulis, S.; Frazier, K.; Verhagen, J.; Zhang, Y.; Iwanowicz, E.; Hendrickson, T.; Knapp, M.; Merritt, H.; Voliva, C.; Wiesmann, M.; Legrand, D.; Bruce, I. WO 2007095588.

²⁴ For compound **6**, rat MX: CL 4 μ g/min/mg, t_{1/2} 187 min; Caco-2: P_{appA-B} (cm/sec x10⁻⁶) 46, P_{appB-A} (cm/sec x10⁻⁶) 42. For compound **9**, rat MX: CL 8 μ g/min/mg, t_{1/2} 778 min;

Caco-2: P_{appA-B} (cm/sec x10⁻⁶) 16, P_{appB-A} (cm/sec x10⁻⁶) 13. For compound **17**, rat MX: CL 8 μ g/min/mg, t_{1/2} 778 min;

Caco-2: P_{appA-B} (cm/sec x10⁻⁶) 40, P_{appB-A} (cm/sec x10⁻⁶) 40.

²⁵ Hamdouchi, C.; Sanchez, C.; Ezquerria, J. *Synthesis*, **1998**, *6*, 867.

²⁶ Structure of compound **17** in PI3K γ submitted under PDB accession code **4KZC**.

